Surface Tension Induced Meniscus Measurement using Free Surface Synthetic Schlieren

Avanish Mishra[1], Varun Kulkarni[1], Jian-Wei Khor[1] and Steve Wereley[1]

[1]School of Mechanical Engineering, Purdue University, West Lafayette, USA

mishra17@purdue.edu

ABSTRACT

Objects lying on the liquid-gas interface create a free surface deformation due to surface tension. In previous studies, it has been shown that capillary/ meniscus interaction between these objects leads to self assembly. This phenomenon is also known as the ‘‘Cheerios effect’’. Surface tension driven self assembly offers an attractive route for creation of highly ordered structures of meso- to microscale entities. A detailed characterization of the self assembly process requires measurement of three dimensional (3d) menisci around the assembling entities. In this work, Free Surface Synthetic Schlieren (FS-SS) method is being used to measure meniscus profile around a vertical glass cylinder submerged in a water pool. The key objective is to analyze the applicability of this method for the measurement of the surface tension induced deformations.

INTRODUCTION

The phenomenon of denser objects floating on a liquid surface is a simple yet fascinating occurrence in nature. We observe this from the common day experience of small floating drawing clips to insects walking on water [1]. More interestingly, a group of such particles placed on a liquid surface tend to coalesce forming a single entity by a process called self assembly. This can be easily visualized by pouring the cereal Cheerios in bowl full of milk and see those lump together [2]. Through these observations the role of surface tension to balance the weight of these objects becomes apparent. A measure of this force opposing the effect of gravity is the extent of liquid surface deformation, commonly referred to as the meniscus. Evaluating the shape of this meniscus by conventional methods is often very restrictive and inaccurate. In this work we propose using the Free Surface Synthetic Schlieren (FS-SS) method [3] which attempts to measure this meniscus accurately, hence eliminating some of the above mentioned difficulties.

Standard methods for measuring surface slope rely on laser beam refraction or reflection [4-7]. The fact that we can achieve only point or line measurements using these procedures implies that they cannot provide instantaneous whole field information. Zhang and Cox [8] attempted to alleviate this problem by using an illuminated color light screen below the water surface to obtain the whole field surface deformation. They imaged this screen through deformed water surface via a collimating lens submerged in water. The captured images of color pattern were processed to determine surface gradient. This method suffers from complex setup requirements due to the necessity of a collimating lens. The techniques employing scattered light in place of collimated light considerably simplify the optical setup. Free Surface Synthetic Schlieren (FS-SS) method developed by Moisy et al. [3] utilizes scattered light. It is based on the work done by Kurata et al. [9] and Elwell [10]. Kurata et al. [9] measured three dimensional profile of shallow water surface using a novel optical method in which a grating was placed below the water tank. The grating acted as point sources of light and two images were recorded, one with plane water surface and other with surface waves. Both the images were then compared with each other and feature movement between the images was determined. Based on the geometrical optics, feature displacement was related to water surface height. Elwell [10] used a similar method to measure surface deformation produced by vortices in a shallow water tank. However, instead of using grating he visualized a back-illuminated speckle pattern of dots printed on paper to reduce possibility of optical aliasing. Free Surface Synthetic Schlieren method utilizes same setup as that of Elwell [10]. Simplicity of the method lies in the fact that it does not require any collimating optics and it can be easily configured for a wide variety of problems.

EXPERIMENTAL METHODS

Figure 1 and 2 show the schematic diagram and a photograph of the experimental setup, respectively. In this method, a background speckle pattern was first imaged through an undistorted plane surface of water pool, as shown in Figure 3 (a). After that a glass cylinder of 0.87 mm was inserted in the water pool and the same background pattern was imaged through the surface tension induced meniscus, as shown in Figure 3(b). The images were acquired using a Nikon DS-Fi1 camera and the background illumination was provided by X-Cite 120 PC lamp, as shown in Figure 2. The deformations in the free surface lead to an in plane shift of background pattern between Figure 3(a) and 3(b). This in plane displacement can be computed by PIV cross correlation algorithm. In present work, a commercial PIV code LaVision DAVIS 7.2 was used for the computation of the displacement field. At first, both the images were processed using a high pass filter with a scale length of 150 pixels. It filtered out intensity fluctuations in the background. Subsequently, vector field was computed in multipass mode with decreasing window sizes. The cross correlation was started with a window size of 128×128 pixel^2 with 50% overlap and finally reduced to a window size of 64×64 pixel^2 with 75% overlap. Two iterations were performed for each window size. During postprocessing, vectors with peak ratio less than 1.2 were deleted. A median filter with strongly remove and iteratively replace option was used.

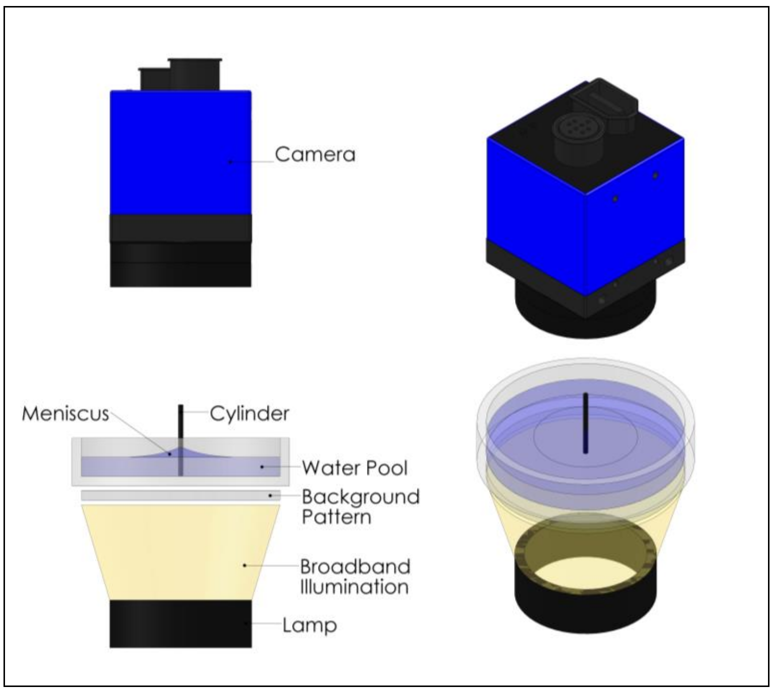

Fig 1: Schematic of the Experimental Setup.

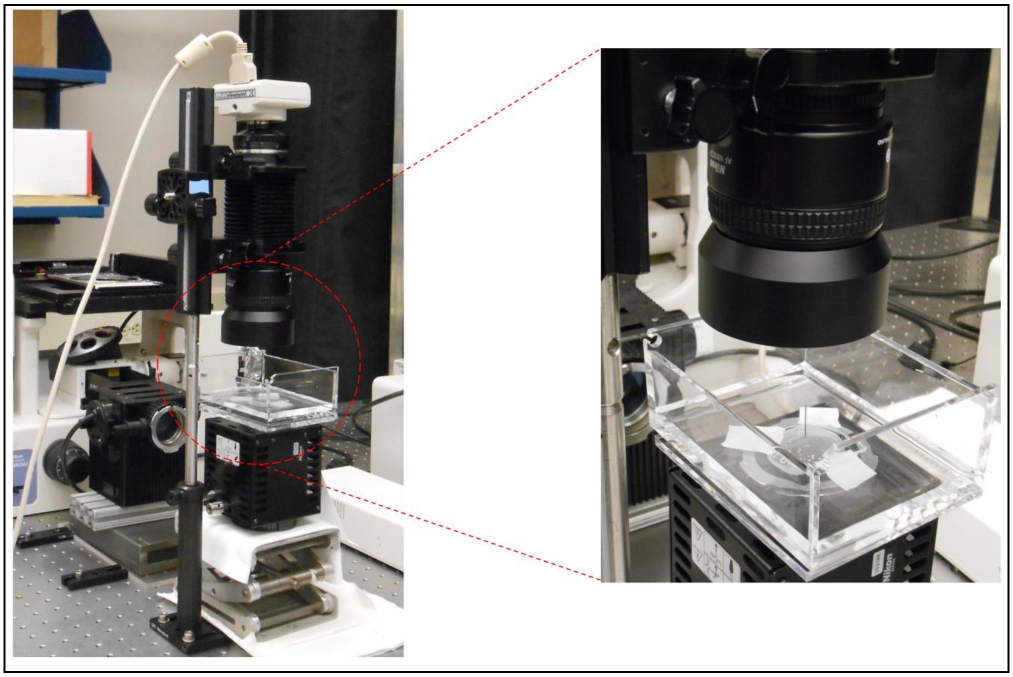

Figure 2: Photograph of the Experimental setup

Vectors were removed if difference to median is greater than twice the root mean square of neighbors while vectors were reinserted if difference to median is less than thrice the root mean square of neighbors. During the application of median filter, groups with less than five vectors were removed. Finally removed vectors were filled by interpolation. The vector calculation in the circular rod and highly deformed region around it was masked by a mask as shown in Figure 4. The FS-SS method requires surface gradient to be small but meniscus close to the circular rod is very steep. The high surface gradient close to the circular rod leads to large deformation in the background image. Hence, both circular rod and adjacent region were masked.

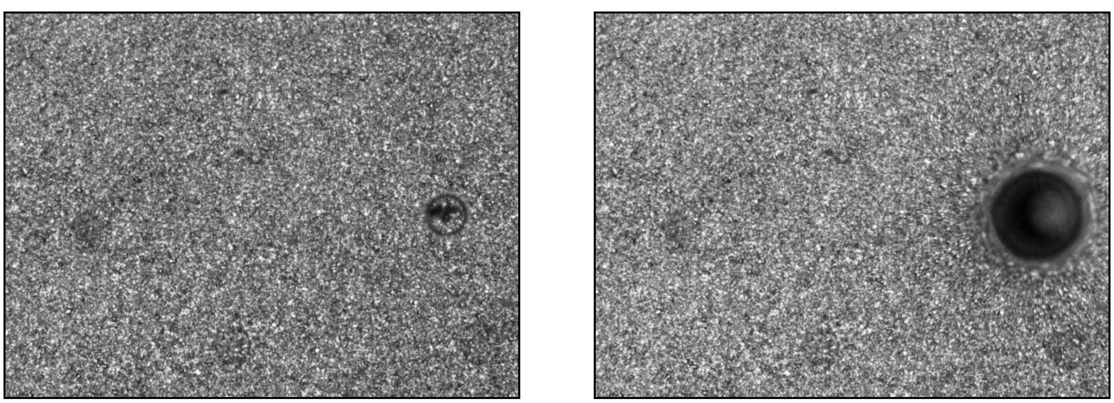

Figure 3 (a) Background pattern images through the plane and (b) deformed interface, respectively.

The computed displacement vector field was eventually processed using ‘surfheight’ function in PIVMAT toolbox developed by Moisy [11] to generate 3d profile of the meniscus which is shown in Figure 5. The test liquid used was D.I. Water and its density was measured to be 998 ± 3 kg/m^3.

It is important to compare the measured 3d profile of the meniscus with the numerical solution for validation. However, numerical solution of meniscus profile around a vertical cylinder requires the contact angle to be known. The contact angle was measured to be 55˚ from a side view image of the meniscus profile, as shown in Figure 6. The surface tension of the D.I. water/air interface was measured to be 72.8 ± 2 mN/m by using Wilhelmy plate Krüss tensiometer. Procedure of the numerical solution is being described in the next section.

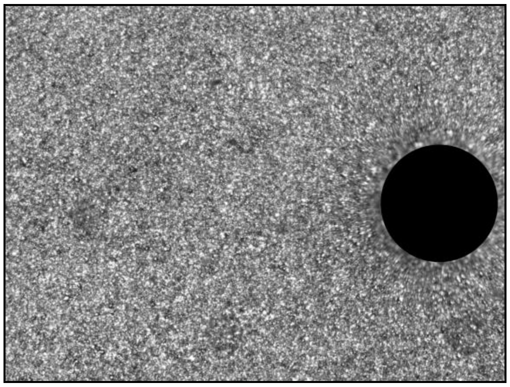

Figure 4: Mask

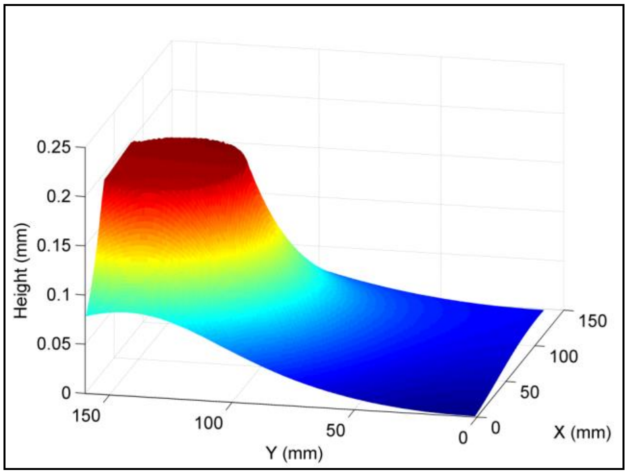

Figure 5: Measured three dimensional profile of the meniscus.

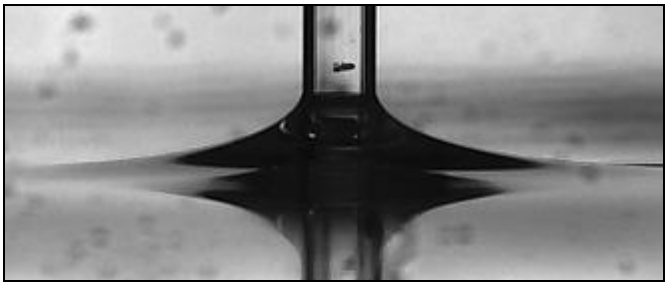

Figure 6: Side view image of the meniscus profile, Contact Angle = 55˚.

NUMERICAL SOLUTION

To obtain the meniscus profile we need to solve the Young–Laplace equation for the axisymmetric case [12] which can be written as,

$$\frac{\mathrm{d}^2 z}{\mathrm{d}x^2} = \left[1+\left(\frac{\mathrm{d}z}{\mathrm{d}x}\right)^2\right]\left\{\frac{\rho_l \mathrm{g}}{\sigma_{al}} z \left[1+\left(\frac{\mathrm{d}z}{\mathrm{d}x}\right)^2\right]^{1/2} - \frac{1}{x}\frac{\mathrm{d}z}{\mathrm{d}x}\right\} \tag{1.1}$$

with boundary conditions,

$$\frac{\mathrm{d}z}{\mathrm{d}x} = -\tan\theta_{\mathrm{c}} \quad \text{at} \quad x = r_0 \tag{1.2}$$

$$y \to 0 \quad \text{at} \quad x \to \infty \tag{1.3}$$

The variables used above are illustrated in Figure 7.

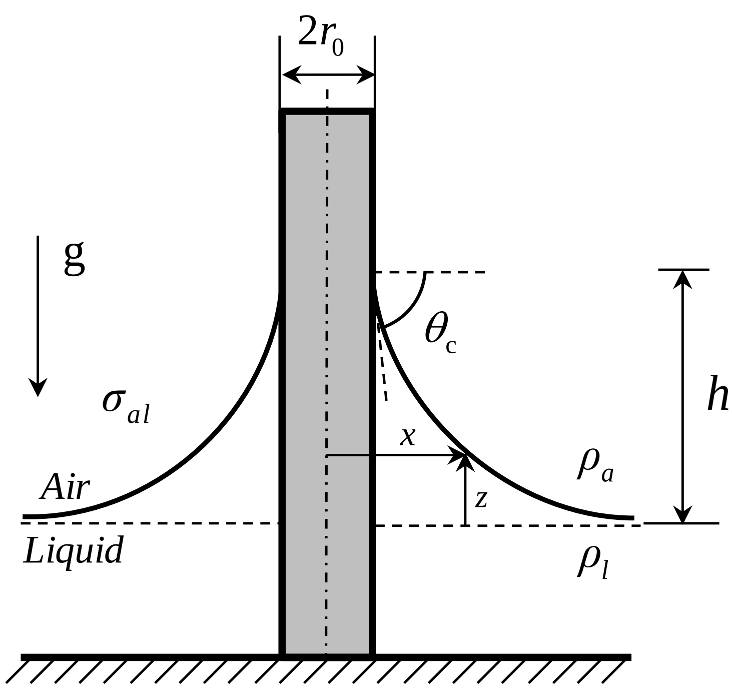

Fig 7: Sketch of the vertical cylinder with the liquid meniscus and coordinate axes.

Equation (1.1) can be solved numerically by shooting method and using secant updates. However, by non-dimensionalising (1.1) using the two length scales: the radius of the cylinder, r_0 and the capillary length ℓ_{c} we can obtain analytical solutions close to the cylinder and far from it. These solutions are obtained using the method of matched asymptotic expansions. Details of the procedure can be found in [12]. For the sake of brevity we represent the key results below.

Inner solution y_{inner} is,

$$y_{inner} = -\sin\theta_c\left(ln\,\varepsilon\right) + \sin\theta_c\left(2ln\,2 - \gamma\right) - \sin\theta_c\, ln\left[r + \left(r^2 - \sin^2\theta_c\right)^{1/2}\right] \tag{1.4}$$

Where, $\varepsilon = r_0/\ell_c$ capillary length, $\ell_c = \sqrt{\dfrac{\sigma_{al}}{\rho_l\, g}}$, $y = z/r_0$, $r = x/r_0$

Outer solution y_{outer} is,

$$y_{outer} = \sin\theta_c\; K_0\left(R\right) \tag{1.5}$$

$K_0(R)$ is modified Bessel function of order zero, $y = z/r_0$ and $R = x/l_c$

Height of the meniscus, h, at the cylinder boundary is obtained using (1.4),

$$h = r_0 \sin\theta_c \left\{ ln\left[\frac{4}{\varepsilon\left(1+\cos\theta_c\right)}\right] - \gamma \right\} \tag{1.6}$$

Here, γ is the Euler–Mascheroni constant (= 0.5772).

Equation (1.6) is particularly important as it obviates the need for shooting. With (1.6) the boundary condition at infinity may not be imposed and the boundary value problem can be converted to an initial value one. To numerically solve (1.1) we convert it to a system of ordinary differential equations (as represented in a matrix form) in (1.7) and then use the Euler method.

$$\begin{bmatrix} dz_1/dx \\ dz_2/dx \end{bmatrix} = \begin{bmatrix} 0z_1 + z_2 \\ \left\{1 + \left(dz_1/dx\right)^2\right\}\left\{\dfrac{\rho_l g}{\sigma_{al}} z_1 \sqrt{1+z_1^2} - \dfrac{z_2}{x}\right\} \end{bmatrix} \tag{1.7}$$

Figure 8 compares axisymmetric meniscus profile from FS-SS with numerically determined meniscus profile. It shows that FS-SS can measure 3D profile of the surface tension induced meniscus as long as surface gradients are not large. Close to the cylinder the surface gradients are steep hence meniscus profile cannot be measured experimentally at that location. However further away we are accurately able to obtain the profile.

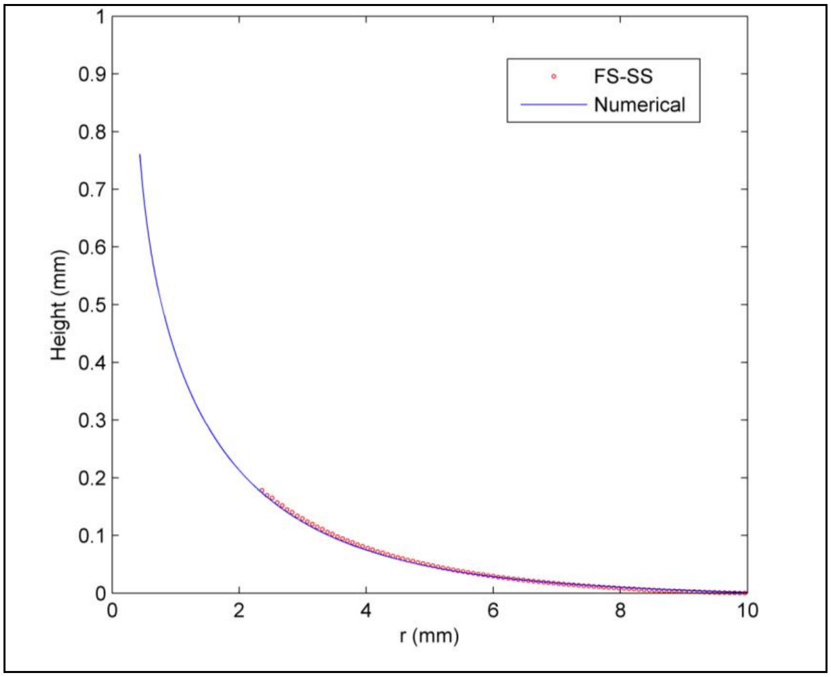

Figure 8: Numerical and experimental meniscus profile

SUMMARY AND CONCLUSIONS

In this work we demonstrated the applicability of FS-SS for measuring surface tension induced deformations. As a test case meniscus around a vertical rod immersed in D.I. Water was studied. The experimental profile of the meniscus was determined from the FS-SS while numerical solution was determined by solving the Young–Laplace equation for the axisymmetric case. Both the results were found to be in excellent match with each other. It clearly proves that FS-SS method can be used for accurate determination of meniscus profile as long as surface gradients are not steep. In future, authors expect to use this method for studying meniscus evolution during self-assembly process.

NOMENCLATURE

r_0 – radius of the cylinder (m)

θ_c – contact angle (rad)

h – the height of meniscus at tube boundary (m)

ρ_a – density of air (kg/m^3)

ρ_l – density of liquid (kg/m^3)

σ_{al} – surface tension of the air/liquid interface (N/m)

g – gravitational acceleration (= $9.81 m/s^2$)

REFERENCES

[1] Vella D., 2007, The Fluid Mechanics of floating and sinking, PhD thesis, University of Cambridge

[2] Vella D., Mahadevan L., 2005, American Journal of Physics, 73, 817–825

[3] Moisy, F., Rabaud, M., and Salsac, K., Experiments in Fluids, 2009, 46, 1021–1036

[4] Tober G., Anderson R. C., Shemdin O. H., 1973, Applied Optics, 12 (4), 788–794

[5] Lange P. A., Ja¨hne B., Tschiersch J., Ilmberger I., 1982, Review of Scientific Instruments, 53:651

[6] Liu J., Paul J. D., Gollub J. P., 1993, Journal Fluid Mechanics, 250, 69–101

[7] Savalsberg R., Holten A., van de Water W., 2006, Experiments in Fluids, 41, 629–640

[8] Zhang X., Cox C. S., 1994, Experiments in Fluids, 17, 225–237

[9] Kurata J., Grattan K.T.V., Uchiyama H., Tanaka T., 1990, Revew of Scientific Instruments, 61 (2), 736

[10] Elwell F.C., 2004, Flushing of embayments, PhD thesis, University of Cambridge

[11] Moisy, F., http://www.fast.u-psud.fr/pivmat/

[12] Lo L.L., 1983, "The meniscus on a needle – a lesson in matching", Journal of Fluid Mechanics, 132, 65-78